Magnetic resonances verified in agreement with an assumed time-asymmetric evolution

H. G. Weber and G. Miksch
Physikalisches Institut, Universität Heidelberg, D-6900 Heidelberg 1, Federal Republic of Germany
(Received 11 October 1984)

With use of a narrow-band laser, the free NO_2 molecule is prepared in a well-defined excited state under conditions that correspond to an optical-frequency—radiofrequency double-resonance experiment. We observe a resonant increase or decrease (dependent on the divergence of the light beam) of the total fluorescence intensity when the radiofrequency field is in resonance with the Zeeman splitting in the ground or excited state of the laser-induced transition. These resonances differ significantly from well-known optical-rf double-resonance signals and laser saturation effects. The resonances are, however, well described with use of a model which assumes an irreversible evolution in the free NO_2 molecule.

I. INTRODUCTION

In a previous paper (Ref. 1) we reported on a new effect, called inversion effect. It is observed when the small polyatomic molecule NO_2 is prepared into a single and well-defined excited state by light absorption. As the intensity of the exciting laser light is varied, the degree of polarization of the fluorescence light may undergo a change in sign. This result is unexpected. It cannot be explained conventionally, as we showed in Ref. 1.

In the present paper we report on a different experiment. Also, this experiment confronts us with an unexpected result which in our opinion cannot be explained conventionally. The experiment is as follows. Using a narrow-band laser and molecular-beam conditions, the free NO_2 molecule is prepared into a well-defined excited state under conditions that correspond to an optical-frequency—radiofrequency double-resonance experiment. Because of the high selectivity in the excitation process and the sparse level structure of the molecule we expect a situation similar to atoms, namely, preparation of the molecule into a single, isolated quantum state and the subsequent radiative decay of this prepared state. However, the experimental results contradict this belief. The results are confronting us with a property of the optically excited state which has no analogy in atomic physics. We observe a resonant increase or decrease (dependent on the divergence of the light beam) of the total fluorescence intensity when the radiofrequency field is in resonance with the Zeeman splitting in the ground or excited state of the laser-induced transition. These resonances differ significantly from conventionally known optical-rf double-resonance signals and laser saturation effects.

In the accompanying paper (Ref. 2) we present a model which describes the inversion effect and the results of the present experiment consistently. However, this model needs a strong assumption. It assumes a time-asymmetric intramolecular evolution in the optically excited molecule. No alternative explanation of the experimental results could be found.

II. EXPERIMENTAL

A schematic diagram of the experimental apparatus is shown in Fig. 1. Light from a single-mode cw dye laser propagates along the **x** axis. The laser light excites NO_2 molecules propagating freely in a molecular beam along the **z** axis. A photomultiplier detects the molecular fluorescence emitted along the **y** axis. The detection is insensitive to the polarization of the fluorescence light. A static magnetic field B and a radiofrequency field can be applied. The static magnetic field is directed along the **z** axis. The rf field is linearly polarized with the magnetic field being directed parallel to the **x** axis. In the experiments the laser light is tuned to a molecular transition near $\lambda = 593$ nm and the fluorescence light is detected unresolved between $\lambda \approx 620$ and 800 nm. The shorter-wavelength limit is set by a color filter in the fluorescence detection path. The longer-wavelength limit is set by the sensitivity of the photomultiplier.

The following experiments are performed.

(i) The B field is parallel to the **z** axis and is swept through a chosen field value B_0 which satisfies the resonance condition $2\pi\hbar\nu_s = g\mu_B B_0$ where $\nu_s = \omega_s/2\pi$ is the

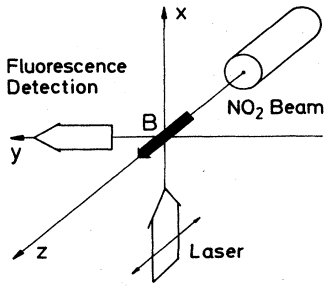

FIG. 1. Geometrical arrangement of the experimental apparatus [arrangement (i)]. The radiofrequency field is not indicated.

constant frequency of the rf field, and $\hbar$, μ_B, and g are the Planck constant, the Bohr magneton, and a g factor belonging to one of the states involved in the laser-induced transition. The laser beam is linearly polarized parallel to the z axis. This excitation condition is usually named π-polarized excitation. It involves transitions between sublevels having the same m quantum numbers in the ground and electronically excited state.

(ii) The experimental conditions are the same as in (i) except that the laser light in linearly polarized parallel to the y axis. This excitation condition is usually named σ-polarized excitation, involving transitions with $\Delta M=\pm 1$.

In all experiments we measure the quantity

$$S=(P-P_0)/P_0 \tag{1}$$

vs the magnetic field B which is swept continuously through the desired field value in each experiment. Here P is the fluorescence intensity as seen by the photomultiplier and $P=P_0$ when the magnetic field is off resonance. We realize the measurement of S as follows. The voltage across the photomultiplier is always (for all intensities of the laser light) adjusted to give the same constant output current with the magnetic field being off resonance. This output current is electronically compensated. Only the difference signal is recorded when the magnetic field is swept through resonance. The conditions are the same as described in Ref. 1.

The experimental apparatus is the same as described before (Ref. 1). The only change concerns the laser beam. The laser beam passes a beam expander consisting of two lenses. Varying the distance of the two lenses we can continuously change the divergence of the light beam interacting with the molecules from a divergent to a convergent beam (see Fig. 7). In Sec. III C we describe experiments where we use this possibility. In the experiments described in Secs. III A and III B the divergence of the light beam is as small as possible (the beam is as parallel as possible). Before crossing the molecular beam this light beam passes an aperture whose width d can be varied continuously from 0 to 20 mm. In general we expand the light beam (using different lenses) to the biggest aperture width used in the experiment such that the aperture width d determines the transit time T_L of the molecules through the light field of the laser. The light intensity in the interaction region can be varied by inserting neutral-density filters in the light path.

The transit time T_L is an important quantity in our experiments. To determine $T_L=d/u$ we need to know the aperture width d and the average velocity u of the molecules. To measure the velocity we proceed as follows. The laser beam is split into two beams. One beam is directed along the x axis (perpendicular to the molecular beam). The other beam is directed parallel to the z axis (parallel to the molecular beam). The stray light is suppressed by color filters in the fluorescence detection path. We scan the laser continuously through an absorption line (line $1R$, see below) and record simultaneously the laser-induced molecular fluorescence of both laser beams and frequency marks produced by an external etalon. The two laser beams cause two well-separated fluorescence peaks whose splitting and widths enable us to measure the average velocity component $u=610\pm 25$ ms^{-1} and the velocity spread (half-width at half maximum) $\Delta u=120\pm 10$ ms^{-1} along the z axis.

It is very important to know that the molecules are "free." The pressure in the vacuum system is always less than 10^{-5} Torr. We change the NO_2 stagnation pressure in the nozzle and the distance of excitation of the molecules from the nozzle in the same way as described in Ref. 1. The results reported in the following are independent of these changes.

We perform experiments on several transitions in the NO_2 molecule. In most cases these transitions correspond to the excitation of a single fine-structure level of a single rotational state. A discussion of the level structure of this molecule can be found in Ref. 3. The rotational level structure seems to be well represented by the angular momentum coupling schema $\hat{N}+\hat{S}=\hat{J}$ and $\hat{J}+\hat{I}=\hat{F}$, where $\hat{N}$, $\hat{S}$, $\hat{I}$, and $\hat{F}$ are the rotational, electron spin, nuclear spin ($I=1$), and total angular momentum operators, respectively. In Table I are listed the angular momentum quantum numbers of the ground and excited state of the two transitions (named line 1 and line $1R$) which we studied most. Both are transitions to the same excited state. Line 1 is a P-branch transition ($N+1\rightarrow N$) and line $1R$ an R-branch transition ($N-1\rightarrow N$). Also listed in Table I are the wavelengths in cm^{-1} for these transitions (compare Ref. 1), and the g factors g_F belong to each hyperfine component of the ground and excited state involved in these transitions. The ground-state g factors were calculated from the angular momentum coupling schema $\hat{N}+\hat{S}=\hat{J}$ and $\hat{J}+\hat{I}=\hat{F}$ (see Ref. 4). The excited-state g factors were measured by a double-resonance experiment (Refs. 4 and 5). Below the g factors we add the symbols

TABLE I. Angular momentum quantum numbers and g factors of the two laser-induced transitions mainly investigated.

Transition		Ground state						Excited state					
		q number			g factors g_F			q number			g factors g_F		
Line	cm^{-1}	N	K_a	J	$F=J-1$	$F=J$	$F=J+1$	N	K_a	J	$F=J-1$	$F=J$	$F=J+1$
1	16847.76	2	0	$\frac{5}{2}$	0.561	0.355	0.286	1	0	$\frac{3}{2}$	1.112	0.489	0.400
					B_1	B_2	B_3				A_1	A_2	A_3
$1R$	16850.29	0	0	$\frac{1}{2}$		−0.667	0.667	1	0	$\frac{3}{2}$	1.112	0.489	0.400
						C_1	C_1				A_1	A_2	A_3

A_i, B_i, and C_1 which we will use later on to identify the magnetic resonances associated with these g factors.

III. MEASUREMENTS AND RESULTS

A. Magnetic resonance spectrum

Figure 2 shows the signal S [defined in Eq. (1)] using the experimental arrangement (i) with the laser light tuned to two different absorption lines in NO_2. In both cases the same three hyperfine components of the same excited-state fine-structure level are excited using either line 1 or line $1R$ (see Table I). The resonances appearing in this figure indicate an increase of the total fluorescence intensity by about 5%. In these measurements the divergence of the light beam is as small as possible ($\alpha \approx 0$, see Sec. III C and Fig. 7), the aperture width is $d=3.5$ mm, the light intensity is $I=15$ mW/mm^2, the frequency of the rf field is $\omega_s/2\pi=\nu_s=3.50$ MHz, and the integration time for each signal is about 5 min. The magnetic field values A_i, B_i, and C_1 in Fig. 2 indicate expected magnetic resonances corresponding to the g factors of the ground and excited state on both transitions (see Table I). Similar resonance spectra are obtained on all investigated transitions (about 20) in this molecule. Using the experimental arrangement (ii) instead of arrangement (i) we obtain the same experimental results, a resonant increase of the total fluorescence intensity by about 5% whenever the frequency ω_s of the rf field is equal to the Zeeman splitting of the ground- or excited-state sublevels of the laser-induced transition.

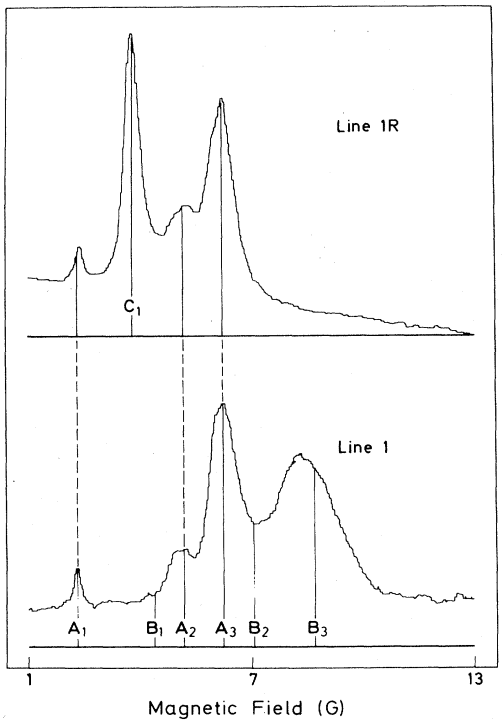

FIG. 2. Magnetic resonance spectrum using the experimental arrangement (i). Line 1 and line $1R$ indicate two laser-induced transitions (P- and R-branch transitions) to the same excited state. A_i, B_i, and C_1 indicate the positions of expected resonances (see Table I).

It must be stated clearly that these resonances are no "ordinary" optical-frequency—radio-frequency double-resonance signals of the kind first observed by Brossel and Bitter (Ref. 6). Ordinary optical-rf double-resonance experiments on the investigated transitions were already reported (Ref. 4). They are detected via a change of the polarization of the fluorescence light, whereas the detection in the present experiments is insensitive to the polarization of the fluorescence light. The width of the ordinary double-resonance signals is about a factor of 20 smaller than the width of the present signals. Using arrangement (ii) we obtain the same resonance signals as with arrangement (i) whereas an ordinary optical-rf double-resonance signal has different signs in arrangements (i) and (ii). We will further note that the resonance A_1 belongs to a state with $F=J-1=\frac{1}{2}$. Using linearly polarized light in the excitation there is no way to observe an ordinary magnetic resonance signal in this state. We name the new resonances in the following "broad rf resonances."

The broad rf resonances appear not always exactly at the expected positions (see A_1 and B_3 in Fig. 2). As a general rule we find that the resonances belonging to hyperfine levels which are connected by the optical transition (see for instance A_1 and C_1 in Fig. 2, line $1R$) seem to attract each other. This effect can well be explained using the model considered in Ref. 2 [see the remark following Eq. (4.2) in Ref. 2]. The effect is strong if the g factors of the ground and excited state involved in the transition are very close or if the experiment is performed at low magnetic B field (i.e., at small frequency ν_s of the rf field). In this case we have a strong overlapping of the broad rf resonances associated with the ground and excited state of the laser-induced transition. However, if the resonances are well resolved there is always good agreement (precision 20%) between the observed and expected position of the resonances on all investigated transitions except on one line, named $2'R$ in Ref. 1. The excited state on this line is $|N=2,J=2-\frac{1}{2}\rangle$ as we know from optical-rf double-resonance and level-crossing experiments (Refs. 4 and 5). The expected ground state is $|N=1,J=1-\frac{1}{2}\rangle$. However, we find a g factor which we have to associate with the ground state $|N=1,J=1+\frac{1}{2}\rangle$. This result demonstrates an interesting application of the new resonances. Obviously they allow us to determine simultaneously the angular momentum quantum numbers of the ground and excited state if the g factor is well behaved. For instance, line $2'R$ seems to be identified as a transition with $\Delta N=1$ but $\Delta J=0$.

Next we consider the widths of the broad rf resonances. The resonances at stronger magnetic fields have a larger width than those at smaller magnetic fields (see for instance B_3 and A_3). The explanation is that (in addition to an influence of the different g factors) at magnetic fields $B>3$ G the splitting of the magnetic sublevels is very nonlinear in B (nonequidistant between the sublevels). This can clearly be seen in ordinary optical-rf double-resonance experiments (Ref. 5). The width of the resonance B_3 is predominantly due to this nonlinear splitting of the magnetic sublevels. On the other hand, strong magnetic fields are necessary to resolve the individual resonances. These conditions restrict, therefore, a detailed

study of these resonances to only few transitions with very different g factors in the ground and excited state. These are transitions involving states with low rotational quantum numbers. For that reason we chose the lines 1 and $1R$ for a detailed study of the new resonances.

The detailed investigation of the broad magnetic resonance at position C_1 reveals that this resonance has a complicated shape if the aperture width d (the transit time) is enlarged to more than 10 mm or for light intensities $I > 10$ mW/mm^2. The resonance changes its shape from a Lorentzian to an approximately Gaussian shape at $d=20$ mm. However for aperture widths $d \leq 8$ mm and light intensities $I \leq 10$ mW/mm^2 the broad rf resonance has a well-defined Lorentzian shape and a clear dependence on the experimental parameters. In this paper we restrict our investigations on the broad rf resonance to these conditions. In Sec. IV C we give an interpretation of the changes observed at larger aperture widths.

The results in Fig. 2 are obtained using an aperture width $d=3.5$ mm. Figure 3 demonstrates how the signal changes if the aperture width d (the transit time T_L) is changed. The measurements are performed on line $1R$ using again the experimental arrangement (i). We summarize the results as follows. The widths of the resonances increase with decreasing aperture width. At $d=1$ mm they grow together to one broad resonance. However, superimposed on this broad resonance there appears a new resonance at position A_3, which is pointing downwards in Fig. 3. This additional resonance which appears at positions A_3 has to be associated with ordinary optical-rf double resonance in the excited state. This was proved as follows. The same experiment is performed using arrangement (ii), i.e., with σ-polarized excitation. The same results are obtained as in Fig. 3 except at position A_3. The additional resonance at position A_3 is pointing upwards in the experimental arrangement (ii). The additional resonance at position A_3 is a "perturbation" caused by ordinary optical-rf double resonance. Magnetic resonance in the excited state does not only affect the polarization of the fluorescence light but also the spatial distribution of the fluorescence light. The additional resonance at A_3 is due to a change in the spatial distribution of the fluorescence light. A similar resonance is expected at position A_2. However, in agreement with results of ordinary optical-rf double-resonance experiments this resonance is much smaller and cannot be seen in Fig. 3.

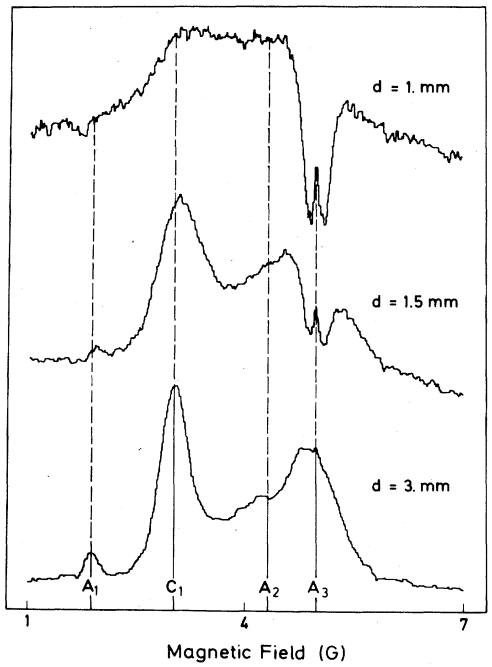

FIG. 3. Magnetic resonance spectrum (line $1R$) using experimental arrangement (i) for different aperture widths d.

The ordinary optical-rf double-resonance signal in Fig. 3 is a superposition of several resonances due to the nonlinear splitting of the magnetic sublevels for $B>3$ G. This determines the width and the shape (the "dip") of this resonance. The ordinary double-resonance signal is always present. However, the dependence of its amplitude on the aperture width d is very different from the dependence of the amplitude of the broad rf resonance on d. As we will show below in more detail, the signal amplitude S of the broad rf resonance increases nearly quadratically with d. On the other hand, the perturbation caused by optical-rf double resonance is approximately independent of d. Therefore, this perturbation vanishes for large aperture widths. The three results in Fig. 3 are not in scale with respect to the signal amplitude. Normalized to the same total fluorescence intensity the signal amplitude S for $d=3$ mm is approximately a factor of 10 larger than the signal amplitude S for $d=1$ mm.

B. The broad rf resonance

In this section we describe in detail the properties of the broad rf resonance. The experiments are performed on the resonance at position C_1 in Fig. 2. This resonance is chosen because it is strong and negligibly disturbed by nearby resonances. The frequency of the rf field is $\nu_s = 1.4$ MHz corresponding to a resonance at $B=1.5$ G. This is found to be the best compromise between the nonlinearity in the Zeeman splitting and the attainable resolution in the resonance spectrum. It is possible to determine the residual nonlinear magnetic field level splitting using an experimental arrangement with two separated light fields which gives a resolution of less than 5 mG (Ref. 14). From this we obtain a correction of about 5 mG for the half-width at half maximum of this resonance. The shape and width of this resonance depend heavily on the properties of the light beam. In this section we describe experiments in which the light beam is as parallel as possible ($\alpha=0$, see Fig. 7). Under these conditions the broad rf resonance can be well fitted by a Lorentzian shaped curve.

Figure 4 depicts the amplitude and width of the signal S versus the light intensity I of the exciting laser light. In these measurements the aperture width is $d=6.0$ mm and the power of the rf field is kept constant. These results show that the width is independent of the light intensity

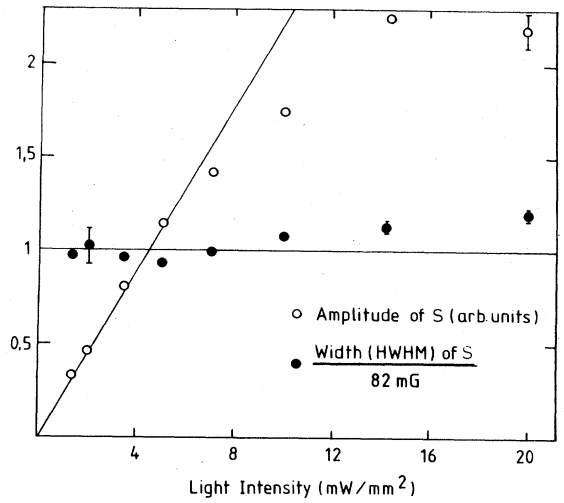

FIG. 4. Amplitude and width (HWHM) of the broad rf resonance [signal S, see Eq. (1)] vs the light intensity.

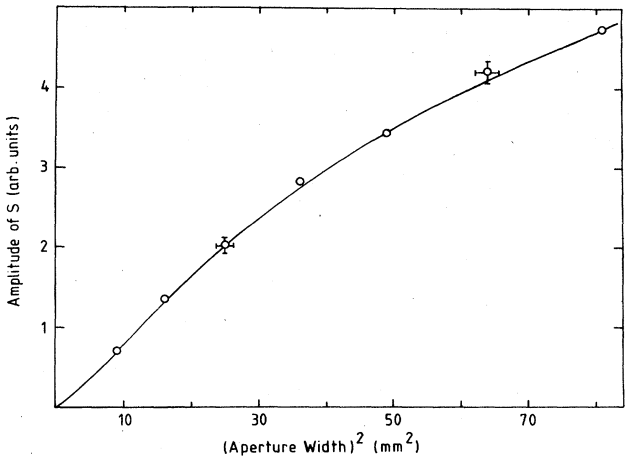

FIG. 5. Amplitude of the broad rf resonance (signal S) vs the aperture width d. Solid line is a theoretical curve.

and the amplitude of S is proportional to the light intensity up to about $I=6$ mW/mm^2. For higher light intensities ($I=20$ mW/mm^2) there is a weak increase of the width up to 20% but a significant deviation of the amplitude S from proportionality to the light intensity by more than 100%. We note that the light intensity $I=I_0$ at which deviations of a linear dependence of S on I appear depend on the aperture width d (the transit time T_L). I_0 decreases with increasing aperture width and vice versa.

Measurements of the amplitude and width of the signal S versus the power of the rf field show results which resemble those in Fig. 4. As a measure for the rf-field power we use the square of the peak-to-peak voltage V_{ss} across the rf coils. A voltage of $V_{ss}=10$ V corresponds to a magnetic field strength of the rf field of about 250 mG at the resonance frequency $\nu_s=1.4$ MHz. The results show that for aperture widths $d\leq 6$ mm the width is independent of the rf-field power and the amplitude is proportional to the rf-field power up to $V_{ss}=V_{ss}^0\approx 50$ V. For higher voltages the width increases also of the order of 20% and the amplitude is below the linear dependence on the rf-field power. If the aperture width is increased the limiting voltage V_{ss}^0 is below 50 V.

Figure 5 depicts the amplitude of the signal S versus the square of the aperture width d, and Fig. 6 depicts the half-width at half maximum (HWHM) of the signal S versus $1/d$. In both cases the light intensity is $I=2.5$ mW/mm^2 and the power of the rf field corresponds to $10V_{ss}$. In both figures the dots represent experimental results and the solid lines theoretical curves which will be explained in Sec. IV B.

Molecular-beam conditions allow an additional experiment which cannot be performed under static gas conditions. Because the lifetime of the molecules in the excited state is about 30 μs the molecules travel on the average more than 1 cm after excitation before they decay radiatively. In general we work with equal detection sensitivity over a path length of at least 5 cm including the region of excitation of the molecules. However, it is also possible by using suitable spatial filters in the fluorescence detection path to selectively detect the fluorescence light coming from the spatial region near the excitation volume only (we name this detection position 1) or for instance fluorescence light which is emitted from molecules which traveled at least 1 cm after excitation (we name this detection position 2). At first we perform a Hanle experiment because its width is not rf field power-broadened as in the optical-rf double-resonance experiment (Refs. 4 and 5). As expected, the Hanle signals in detection position 2 have a much narrower width than those obtained in detection position 1. This is so because in detection position 1 we select molecules with a short radiative lifetime and in detection position 2 we select molecules with a long radiative lifetime. We perform the same experiments with the broad rf resonance. There appears no difference in the width of both resonances in detection positions 1 and 2. This demonstrates that the width is not dependent on the

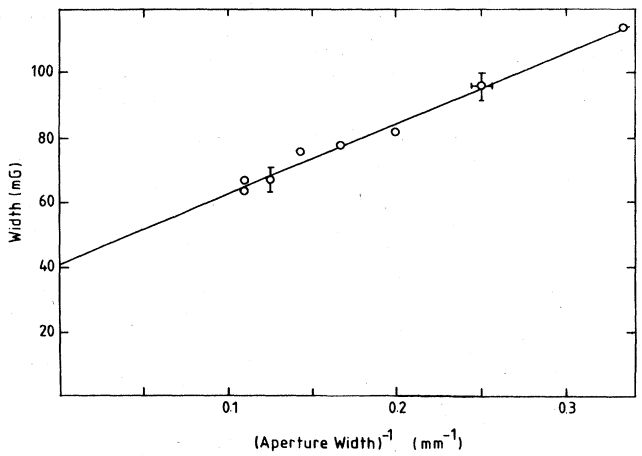

FIG. 6. Width of the broad rf resonance vs the aperture width d.

lifetime of the radiatively decaying state.

The broad rf resonance at position C_1 has to be associated with the ground state of the laser-induced transition. We investigate also the resonance at position A_1 which has to be associated with the excited state of the laser-induced transition. The results on resonance A_1 are not as precise as those on resonance C_1. However, we have no indication that the resonance at A_1 behaves differently from the resonance at C_1.

C. Effect of light beam divergence

In this section we describe the influence of the divergence of the light beam on the broad rf resonance. We characterize the divergence by an angle α (see Fig. 7). In the experiments considered before the light beam is as parallel as possible (divergence $\alpha=0$). Experimentally this is achieved by adjusting the distance between the two lenses in the beam expander. This distance can continuously be changed to produce a diverging ($\alpha=2$ mrad) or a converging ($\alpha=-2$ mrad) light beam. The divergence α causes a relative Doppler shift of the different components of the light field as seen by the molecules. A calculation with the velocity component along the z axis $u=610$ ms^{-1} shows that the divergence $|\alpha|=1$ mrad corresponds to a maximal relative Doppler shift 1.0 MHz. In the following experiments we use no aperture in the light beam (the entrance window into the vacuum chamber has a diameter of 5 cm) and the overall light intensity is kept constant. The laser is tuned to line $1R$. For $\alpha=0$ the laser beam has an elliptical sectional area with about 3 mm parallel to the molecular-beam axis and about 2 mm perpendicular to the molecular-beam axis.

The first observation we report here is the dependence of the total fluorescence intensity on the angle α. No rf field is used, and the results show no significant dependence on the magnetic field B. We record the total fluorescence intensity versus the angle α. Independent of the overall intensity of the light beam the total fluorescence intensity has always a minimum for $\alpha=0$. For strong light intensities ($I\geq 400$ mW) the fluorescence intensity increases by about a factor of 2 if we vary α from $\alpha=0$ to $|\alpha|=2$ mrad. The dependence on α is to a good approximation symmetric around $\alpha=0$. We note that the molecular beam is an effusive beam. No collimation is used. At the position where the molecules are excited in the beam the molecular beam has presumably a "diameter" which is large compared to the laser beam diameter even in the case of the divergent light beam. The strong dependence of the total fluorescence intensity on $|\alpha|$ offers a convenient and very efficient (precision ≤ 0.1 mrad) method to adjust the divergence of the light beam to a minimum.

The experiments we are reporting now are measurements of the broad rf resonance for different values α. Figure 8 shows results using the experimental arrangement (i) with the frequency $\nu_s=1.0$ MHz of the rf field. Results for three different values α are depicted. For $\alpha=0$ the result is in agreement with those reported in Secs. III A and III B (see, for instance, Fig. 3). The expected positions for the resonances A_1, A_2, A_3, and C_1

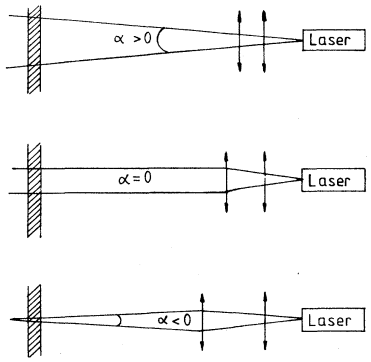

FIG. 7. Experimental arrangement to investigate the influence of divergence of the light beam on the broad rf resonance. Two lenses are indicated which allow to change α continuously. Hatched area represents the molecular beam.

are indicated in this figure. However, the broad rf resonances in Fig. 8 are not resolved because the frequency of the rf field is too low. This causes a strong overlapping of the individual resonances. Moreover, this overlapping results also in a shift of these resonances (an attraction) as mentioned in Sec. III A. At position A_3 we see also a strong perturbation which we attribute to optical-rf double resonance in the excited state (see discussion below). The two other results shown in Fig. 8 are measurements with a diverging light beam ($\alpha=2$ mrad) and with a converging light beam ($\alpha=-2$ mrad).

Disregarding smaller details both results for $|\alpha|=2$ mrad are the same. They differ significantly from the result for $\alpha=0$. For $\alpha=0$ the broad rf resonances represent a resonant increase of the total fluorescence intensity, and the results for $|\alpha|=2$ mrad indicate a resonant decrease of the total fluorescence intensity. Altering $|\alpha|$ continu-

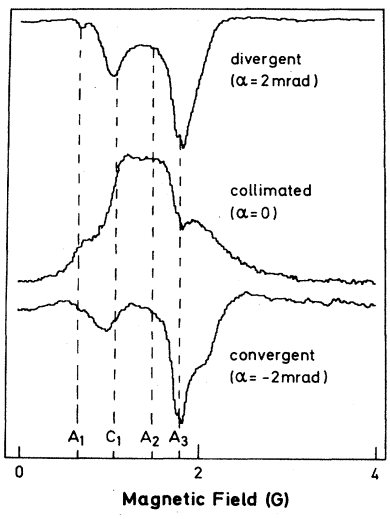

FIG. 8. The broad rf resonance for three α values. α designates the divergence of the light beam (see Fig. 7).

ously from $\alpha=0$ to $|\alpha|=2$ mrad we observe the following. Increasing $|\alpha|$ causes a decrease and finally a total disappearance of the broad rf resonances studied in Secs. III A and III B. At a given divergence $|\alpha|=|\alpha_0|>0$ new resonances appear near the positions A_1, A_2, A_3, and C_1. The new resonances are not an "inversion" of the resonances for $\alpha=0$. They have a different shape and a different width. They are also often shifted with respect to the expected position in a different way than the resonances for $\alpha=0$. These resonances increase approximately proportional to $|\alpha|$ for $|\alpha|>|\alpha_0|$ in the investigated range of the α values. α_0 itself increases with the frequency of the rf field and therefore with the splitting of the magnetic sublevels on resonance, such that the relative Doppler shift associated with α_0 agrees approximately with half the frequency of the rf field. Other properties of the new resonances are as follows. Their amplitude [the amplitude of S, see Eq. (1)] increases proportional to the intensity of the laser light and approximately also proportional to the power of the rf field. Their widths seem to be independent of the light intensity and of the rf field power. In general these resonances are small compared to the resonances for $\alpha=0$. The signals shown in Fig. 8 are not in scale. The signal amplitude of the resonances for $|\alpha|=2$ mrad is about a factor of 5 smaller than the signal amplitudes of the resonances for $\alpha=0$.

There are also differences between the resonances for $\alpha>0$ and $\alpha<0$. In both cases the resonances increase with increasing $|\alpha|$, however, for $\alpha>0$ about 30% stronger than for $\alpha<0$. The widths of the resonances are different in both cases. Also the resonances are shifted with respect to the expected position in a different way. We do not investigate these differences in detail here. We note only that the transit time of the molecules in the light field is very different for $\alpha>0$ and $\alpha<0$.

The resonance at position A_3 is perturbed by optical-rf-double resonance in the excited state as already pointed out in Sec. III A. (compare the results in Fig. 3). In the present experiment this perturbation is even stronger. This is probably due to the weaker nonlinearity in the Zeeman splitting in the present case. This increases the optical-rf double-resonance signal but not the broad rf resonance signal. This perturbation appears as downward directed resonance in Fig. 8 because we use π-polarized excitation [arrangement (i)]. Therefore the perturbation lowers the resonance signal for $\alpha=0$ at the right wing. On the contrary, for $|\alpha|=2$ mrad the perturbation adds to the already downward-directed broad rf resonance signal. At least 50% of the resonance at position A_3 for $|\alpha|=2$ mrad are caused by this perturbation. We also perform experiments with arrangement (ii), i.e., with σ-polarized excitation. The broad rf resonances for $\alpha=0$ and $|\alpha|>|\alpha_0|$ behave in both experimental arrangements alike. However, in arrangement (ii) the perturbation by optical-rf double resonance gives an upward directed resonance opposite to the arrangement (i). We note also that the perturbation by optical-rf double resonance appears strongly power-broadened in Fig. 8.

The changeover of the broad rf resonance from a resonant increase to a resonant decrease of the total fluorescence intensity versus the divergence of the light

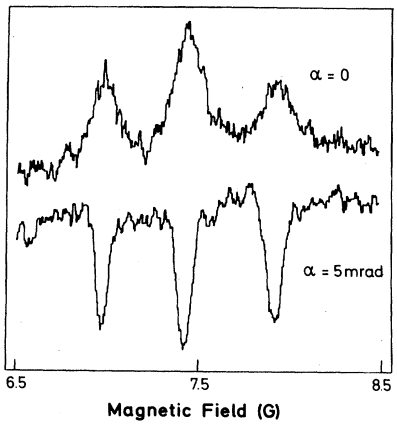

FIG. 9. The broad rf resonance for two α values at high magnetic field (resonance at position C_1, see text). α designates the divergence of the light beam (see Fig. 7).

beam is in our opinion a novel observation. In Fig. 9 we give an additional example of this effect. The experimental conditions are as follows: experimental arrangement (i), $\nu_s=7.0$ MHz (the maximum rf field frequency possible in our experiment), and a total light intensity of 400 mW of the laser. For $\alpha=0$ the aperture width (the transit time) is $d=5$ mm. For $\alpha=2$ mrad we find no resonance signal. The experimental apparatus had to be changed making bigger values of α possible. With $\alpha\approx 5$ mrad we obtain the downward-directed resonances shown in Fig. 9. We note that the averaging time is about 2 min for the signal with $\alpha=0$ and about 10 min for the signal with $\alpha\approx 5$ mrad. In Fig. 9 only the resonance at position C_1 is shown. However, the magnetic field is now so strong that the magnetic resonances between the ground-state levels $|F=\frac{3}{2},m\rangle$ with $m=\pm\frac{1}{2},\pm\frac{3}{2}$ yield three separate resonances of which the resonance associated with the rf field transition $|F=\frac{3}{2},m=\frac{1}{2}\rangle\leftrightarrow|F=\frac{3}{2},m=-\frac{1}{2}\rangle$ coincides with the resonance associated with the rf-field transition $|F=\frac{1}{2},m=\frac{1}{2}\rangle\leftrightarrow|F=\frac{1}{2},m=-\frac{1}{2}\rangle$.

IV. DISCUSSION

A. Stabilization versus saturation

A broad rf resonance structure superimposed on the expected optical-rf double-resonance spectrum was already observed before in optical-rf double-resonance experiments on NO_2 (Refs. 7 and 8). However, no satisfying explanation of this resonance structure could be given. Only when the inversion effect was observed did it become immediately clear that the broad rf resonance is intimately connected with this effect (Ref. 9). In Ref. 8 an effort was made to associate the broad rf-resonance structure with optical saturation resonances in radiofrequency dressed molecules. An agreement of the experimental results with the saturation resonances could not be excluded because the broad rf-resonance structure remained unresolved. The effect of the transit time T_L (see Fig. 3, for

instance) was not recognized. The present experiments reveal, however, a property of the broad rf resonances which to our opinion cannot be explained by any known laser saturation effect (see, for instance, Refs. 10—12). This property is the change over of the broad rf resonance from a resonant increase to a resonant decrease of the total fluorescence intensity versus the divergence of the light beam. But also other properties of the broad rf resonance, i.e., the dependence on the light intensity and on the transit time T_L are difficult to explain by the known laser saturation effects. We conclude therefore that the broad rf resonance is a novel phenomenon.

According to Sec. II the conditions of the experiments are such that to all our knowledge a NO_2 molecule is prepared under collision-free conditions into a single, isolated and well-defined quantum state and the fluorescence decay of this prepared state is observed. However, the experimental results are in contradiction to this knowledge because the results of Sec. III cannot be explained for such a system. In Ref. 1 we were confronted with a similar situation. A consistent description of the results in Ref. 1 is possible with the model of light-induced stability of a molecular state (see Ref. 2). In Secs. IV B and IV C we will show that the results of Sec. III can successfully be explained by the same model. This model uses three states $|a\rangle$, $|b\rangle$, and $|c\rangle$ with the magnetic sublevels $|a,m\rangle$, $|b,m\rangle$, and $|c,m\rangle$. Laser light induces a transition from the ground state $|a\rangle$ of the molecule to the excited state $|b\rangle$. However, before $|b\rangle$ decays radiatively the free molecule evolves irreversibly in an intramolecular process from $|b\rangle$ to the state $|c\rangle$. The fluorescence decay of $|c\rangle$ is observed. In Ref. 2 we evaluate the quantity $P=\sum_m \rho_{cc}^{mm}$ where ρ_{cc}^{mm} is the occupation probability of the sublevel $|c,m\rangle$. Thus P represents the total occupation probability of the state $|c\rangle$. The broad rf resonance is evaluated for the quantity $S=(P-P_0)/P_0$, with $P=P_0$ when the magnetic field is off resonance. In the following we compare this quantity with the signal S introduced in Eq. (1) of this paper. Both quantities are equal if we neglect spatial asymmetries in the fluorescence light. However, spatial asymmetries are present as we already pointed out in Sec. IV. They are mainly connected with the ordinary optical-rf double-resonance signal. They appear as perturbations on the broad rf resonance (see Fig. 3 for instance). Spatial asymmetry in the fluorescence light may also appear with the broad rf resonance studied here. This is so, because the stabilization effect (see Ref. 2) causes also differences in the occupation probabilities ρ_{cc}^{mm}. The differences in the ρ_{cc}^{mm} result in broad rf resonances in the polarization-sensitive detection of the fluorescence light. These are actually the broad rf resonances first observed in Refs. 7—9. Differences in the ρ_{cc}^{mm} are also connected with a spatial asymmetry of the fluorescence light. This effect is certainly smaller than the perturbation caused by optical-rf double resonance and we neglect it here.

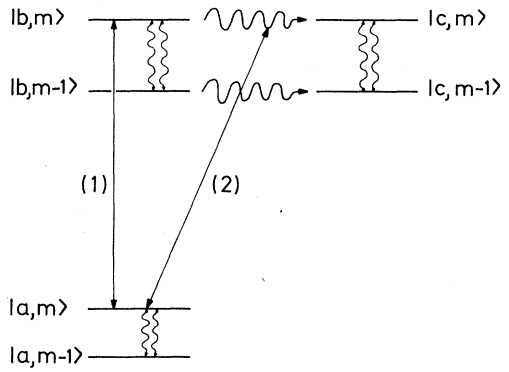

FIG. 10. Schematic diagram for the explanation of the broad rf resonance (see text). Vertical wavy lines indicate interactions caused by the rf field.

B. The broad rf resonance

In this section we discuss the broad rf resonance under the conditions of beam divergence $\alpha=0$. Equations (4.5)—(4.8) of Ref. 2 predict resonances in the observable S whenever the Zeeman splitting ω_a in the ground state $|a\rangle$ and ω_c in the excited state $|c\rangle$ are equal to the frequency $\omega_s=2\pi\nu_s$ of the rf field. We interpret these resonances according to Ref. 2 as follows. The interaction of a molecule with the light field is separated into two processes (see Fig. 10). First the light field induces a transition [interaction (1) in Fig. 10] between $|a,m\rangle$ and $|b,m\rangle$. The density matrix elements ρ_{bb}^{mm} describing the occupation probability of the sublevels $|b,m\rangle$ are created. Subsequently the molecule experiences an internal evolution which brings it into the state $|c,m\rangle$ (indicated by the wavy line) and simultaneously a second interaction [interaction (2)] with the light field. In Fig. 10 the interaction (2) is indicated between the states $|a,m\rangle$ and the wavy line connecting $|b,m\rangle$ and $|c,m\rangle$. There is no transition dipole moment between $|a\rangle$ and $|c\rangle$. Interaction (2) slows down the evolution of the molecule from $|b,m\rangle$ to $|c,m\rangle$ [see Eqs. (3.5) and (3.6) in Ref. 2]. We call this process light-induced stabilization of the state $|b\rangle$. This process reduces the absorption probability of a molecule and decreases therefore the fluorescence intensity. The effect of a rf field on the stabilization effect is as follows. A rf field which is resonant with the Zeeman splitting in the ground or excited state couples states with the magnetic quantum numbers m and $m\pm1$. This causes a lowering of the stabilization effect (increase of the total fluorescence intensity) if a strong stabilization effect is present (for instance via $\Delta m=0$ transitions) in the absence of the rf field. Equation (4.8) of Ref. 2 gives the following expression for the resonance at $\omega_a=\omega_s$:

$$S_a=\frac{[1-\exp(-\Gamma_{bc}T_L)]}{\Gamma_{bc}}\sum_{m,r}A_m\,|\,G_{ba}^{mm}\,|^2\,|\,B_{aa}^{m\,m+r}\,|^2\frac{(\Gamma_{ac}+b_L)[(\Gamma_{ac}+b_L)^2-x_m^2]}{[(\Gamma_{ac}+b_L)^2+x_m^2]^2\{[x_m+r(\omega_a-\omega_s)]^2+(\Gamma_{ac}+b_L)^2\}}\,. \tag{2}$$

The term $-2x_m r(\omega_a-\omega_s)$ appearing in the numerator of Eq. (4.8) in Ref. 2 is approximated by $+2x_m^2$ because near resonance we have $x_m+r(\omega_a-\omega_s)\approx 0$. The sum in Eq. (2) extends over all magnetic quantum numbers m and $r=\pm 1$. Furthermore, we have $A_m=\rho_{bb}^{mm}(\sum_n \rho_{bb}^{nn})^{-1}$. The matrix elements G_{ba}^{mm} describe the optical transition between the $|a,m\rangle$ and $|b,m\rangle$ and the matrix elements $B_{aa}^{m\,m+r}$ describe rf-field transitions between $|a,m\rangle$ and $|a,m+r\rangle$. $|G_{ba}^{mm}|^2$ is proportional to the intensity I of the exciting laser light and $|B_{aa}^{m\,m+r}|^2$ is proportional to the power of the rf field. The resonance condition for the optical transition is expressed by $x_m=\omega_L-(E_c-E_a)/\hbar - m(\omega_c-\omega_a)$ with $E_c+m\omega_c\hbar$ and $E_a+m\omega_a\hbar$ being the energies of the states $|c,m\rangle$ and $|a,m\rangle$ and ω_L being the frequency of the light field. Γ_{ac} and Γ_{bc} are two phenomenologically introduced decay rates and b_L is the spectral width of the laser light as seen by the molecules during the transit time T_L.

We derived Eq. (2) using several simplifying assumptions (see Ref. 2). The velocity distribution of the molecules is neglected. However, this affects only the transit time T_L because the broad rf resonance is Doppler-free in the same sense as optical-rf double resonance is Doppler-free.

The most important simplification for our present discussion is as follows. The interaction of a molecule with the light field is separated into two independent processes, the interactions (1) and (2) introduced before (see Fig. 10). It is only interaction (2) which appears explicitly in Eq. (2). Therefore the resonance condition for the interaction with the light field is not only given by x_m but is implicitly also contained in A_m.

We consider the situation where the laser beam is well collimated having a divergence $\alpha=0$ as good as possible. We idealize this situation assuming that a molecule sees only a light field having one frequency ω_L. This gives $A_m\neq 0$ if $x_m=0$. We compare, therefore, Eq. (2) under the condition $x_m=0$ with the experimental results described in Sec. III B. In agreement with the experimental results the amplitude of the Lorentzian-shaped signal S_a is proportional to the light intensity and the power of the rf field and the width is independent of the light intensity and of the power of the rf field. As the experimental results in Fig. 6 show, the width (half-width at half maximum) of the resonance is given by

$$\Delta B=41.5\ \text{mG}+\frac{218\ \text{mG mm}}{d} \tag{3}$$

with an error of $\pm 10\%$. With $\Gamma_{ac}+b_L=(\mu_B/\hbar)g\Delta B$ and with $g=0.667$ (see Table I) and $u=610\ \text{ms}^{-1}$ we obtain

$$\Gamma_{ac}+b_L=0.24\ \text{MHz}+\frac{2.1}{T_L}\ . \tag{4}$$

The spectral width b_L of the light field as seen by the molecules is solely given by the transit-time broadening $b_L=2.1/T_L$ because the frequency jitter of the laser light is negligible during the interaction time $T_L\leq 10\ \mu\text{s}$ of the molecules with the light field. We obtain therefore

$$\Gamma_{ac}=0.24\pm 0.03\ \text{MHz}\ . \tag{5}$$

The dependence of the amplitude of S_a on the transit time T_L is also in good agreement with the experimental results. The solid line in Fig. 5 represents a fit of Eq. (2) with $\omega_a=\omega_s$ and $x_m=0$ to experimental data. Using the result in Eq. (4) the fit yields

$$\Gamma_{bc}=0.31\ \text{MHz} \tag{6}$$

with an estimated error of 20%.

For low light intensity and low rf-field power (see the approximation in Ref. 2) Eq. (2) describes the broad rf resonance for $\alpha=0$ in all details. Equation (2) represents only the broad rf resonance in the experimental arrangement (i). It is, however, no difficulty to also evaluate this resonance in the experimental arrangement (ii).

C. Observations for long transit times

We used Eq. (2) to describe the broad rf resonance and assumed implicitly that the quantity $A_m=\rho_{bb}^{mm}(\sum_n \rho_{bb}^{nn})^{-1}$ is independent of the magnetic fields. However, more exactly we need to write $A_m=\rho_{bb}^{mm}[\sum_n \rho_{bb}^{nn}(0)]^{-1}$ where $\rho_{bb}^{nn}(0)$ means ρ_{bb}^{nn} with the magnetic field being far off resonance. We assume again $x_m=0$ and additionally that $B_{aa}^{m\,m+r}$ is independent of m. The signal S_a in Eq. (2) can then be written as a product of the broad rf resonance times the quantity $\sum_m \rho_{bb}^{mm}|G_{ba}^{mm}|^2[\sum_n \rho_{bb}^{nn}(0)]^{-1}$. Also, this quantity increases resonantly if the rf field is in resonance with the Zeeman splitting in the magnetic sublevels because of the following reason. In a given molecule the laser induces with comparable probabilities the transitions $|a,m\rangle\rightarrow|b,m\rangle$ and $|a,m\pm 1\rangle\rightarrow|b,m\pm 1\rangle$ only if $|\omega_b-\omega_a|\leq\Gamma_{ac}+b_L$. This condition is fulfilled at low magnetic fields and short transit times T_L. But in general the laser light is resonant with one of these transitions only (for molecules belonging to one velocity group). We will assume that this is the transition $|a,m\rangle\rightarrow|b,m\rangle$. Molecules in $|a,m\pm 1\rangle$ are not excited if the rf field is off resonance. However, near resonance the rf field induces transitions between $|a,m\rangle$ and $|a,m\pm 1\rangle$ which contribute to the population of ρ_{bb}^{mm} if the laser light has depleted $|a,m\rangle$ significantly. This causes a resonant increase of ρ_{bb}^{mm}. Here we name this effect nonlinear optical-pumping resonance (see also Ref. 13).

The change of the shape of the broad rf resonance (mentioned in Sec. III A) from a Lorentzian to an approximately Gaussian shape for aperture widths $d>10$ mm is in our opinion caused by the above-described nonlinear optical-pumping resonance. For low rf fields (no rf-field power saturation) the nonlinear optical pumping resonance increases proportional to d^2 (up to about $d=20$ mm for our experimental conditions) whereas the broad rf resonance increases less than proportional to d^2 for $d>6$ mm (see Fig. 5). This is the reason why for large aperture widths d the nonlinear optical-pumping resonance contributes strongly to the observed resonance signal. The dependence of the width of the optical-pumping resonance on the transit time (aperture width) is expected to be very different from that observed for the broad rf resonance. Indeed investigations of the observed resonance for $d>10$ mm indicate that the width (HWHM) of the nonlinear

optical-pumping resonance seems to be represented by $\Delta B=0.6(2+d)^{-1}$ G with d in mm. This means that ΔB approaches zero for large values of d as expected. This is very different from the results for the broad rf resonance. We conclude that the nonlinear optical-pumping resonance affects the observed resonance signal only little for measurements with aperture widths $d<10$ mm and light intensities $I<10$ mW/mm^2.

D. Effect of divergence

In this section we discuss the observations connected with the divergence α of the light beam. According to the stabilization effect considered before and as indicated in Fig. 10, the interaction of a molecule with the light field is separated into two processes—interaction (1) and interaction (2). Interaction (1) brings the molecule into the state $|b\rangle$. Subsequently the molecule experiences an internal evolution which brings it into the state $|c\rangle$. This evolution is hindered (stabilization effect) if the molecule experiences simultaneously (during a time of the order Γ_{bc}^{-1}) a second interaction with the light field [see Eqs. (3.5) and (3.6) in Ref. 2]. This decreases effectively the absorption probability. For $\alpha=0$ this effect has a high probability because a molecule which was excited into $|b\rangle$ sees a resonant light field during all its transit time through the light field. The situation is different for $|\alpha|\gg 0$. In this case the probability for a second resonant interaction [interaction (2)] is very poor. Consequently the stabilization effect is very low, because the Doppler effect causes the molecules to go off resonance for the second interaction. The absorption probability is strong. As reported in Sec. III C we observe that the total fluorescence intensity versus the divergence α increases by about 100% if we change α from $\alpha=0$ to $|\alpha|=2$ mrad. If the change in the total fluorescence intensity versus α is caused solely by the stabilization effect then the stabilization effect is really a strong effect.

The broad rf resonance described by Eq. (2) disappears for $|\alpha|\gg 0$. This is seen as follows. The interaction (1) is contained in the term A_m, that is, in the preparation of the matrix elements ρ_{bb}^{mm}. A second interaction with the light field is with high probability off resonant. Therefore $x_m\neq 0$ in Eq. (2). As we see from this equation, S_a disappears for $|x_m|=\Gamma_{ac}+b_L$ and changes the sign if $|x_m|>\Gamma_{ac}+b_L$. However, the resonance conditions $x_m+r(\omega_a-\omega_s)=0$ and $\omega_a=\omega_s$ cannot be fulfilled with $x_m\neq 0$. Therefore the broad rf resonance of the type described in Sec. III B disappears for $|\alpha|\gg 0$.

The derivation of Eq. (2) in Ref. 2 neglects matrix elements $\rho_{bb}^{mm'}$ with $m\neq m'$. Only matrix elements with $m'=m$ are taken into account. This is permissible in the case $\alpha=0$ because the bigger resonance effect seems to be associated with the diagonal matrix elements ρ_{bb}^{mm}. However, in the case $|\alpha|\gg 0$ the resonance associated with the ρ_{bb}^{mm} disappears and a calculation taking into account the matrix elements $\rho_{bb}^{m\,m\pm1}$ is required. This calculation is difficult and we did not perform it. We will, however, show here how the presence of off-diagonal matrix elements $\rho_{bb}^{m\,m\pm1}$ may affect the stabilization effect. We note first that whenever the rf field is in resonance with the Zeeman splitting of the ground or excited state it causes in both cases off-diagonal matrix elements $\rho_{bb}^{m\,m\pm1}$. The stabilization effect [interaction (2)] is now possible for transitions with $x_m=0$ and $x_{m\pm1}=0$ where $x_m=\omega_L-(E_c-E_a)/\hbar-m(\omega_b-\omega_a)$ and $\omega_b=\omega_c$. The transitions with $x_m=0$ and $x_{m\pm1}=0$ correspond to different laser frequencies ω_L and ω_L' which differ by $|\omega_L-\omega_L'|=|\omega_b-\omega_a|$. With ω_L being, for instance, the light frequency in interaction (1) and ω_L' being the light frequency in interaction (2) a stabilization effect is only possible if the rf field is in resonance with the Zeeman splitting of the ground or excited state. We see that in the present case ($|\alpha|\gg 0$) a resonant rf field makes the stabilization effect possible in a situation where it is not possible without a rf field. Furthermore, we see also that for a given frequency of the rf field and therefore for a given value $|\omega_b-\omega_a|$ at magnetic resonance the light-beam divergence must exceed a minimum value because a molecule needs to see light frequencies which differ by $|\omega_b-\omega_a|$.

V. CONCLUSION

There is good agreement between the experimental results described in this paper and the model derived in Ref. 2. Moreover, we see no alternative explanation for the broad rf resonances studied here. Thus we consider the expermental results to be strong support for the equations of motion introduced in Ref. 2.

The broad rf resonance reveals the existence of two characteristic times associated with each optically excited state of the NO_2 molecule. Zero-field level crossing, optical-rf double resonance, and radiative decay measurements yield consistently a lifetime $\tau_R\approx 30$ μs (see Refs. 4, 5, and 15), whereas the broad rf resonance has to be associated with a characteristic time of about 3 μs. This result reveals a remarkable connection with one of the most interesting lifetime problems in molecular spectroscopy, the discrepancy between the lifetime value $\tau_{in}\approx 3$ μs deduced from the integrated absorption coefficient, and the lifetime τ_R obtained from radiative decay measurements.[16] A satisfying explanation of this discrepancy was never obtained. With the results of this paper and the model developed in Ref. 2 a solution of this long-standing problem is indicated.

ACKNOWLEDGMENT

This work was supported by the Deutsche Forschungsgemeinschaft.

[1] H. G. Weber, F. Bylicki, and G. Miksch, Phys. Rev. A **30**, 270 (1984).

[2] H. G. Weber, following paper [Phys. Rev. A **31**, 1488 (1985)].

[3] D. K. Hsu, D. L. Monts, and R. N. Zare, *Spectral Atlas of Nitrogen Dioxide* (Academic, New York, 1978).

[4] F. Bylicki, H. G. Weber, H. Zscheeg, and M. Arnold, J. Chem. Phys. **80**, 1791 (1984).

[5] F. Bylicki and H. G. Weber, J. Chem. Phys. **78**, 2899 (1983).

[6]J. Brossel and F. Bitter, Phys. Rev. **86**, 308 (1952).
[7]H. G. Weber, P. J. Brucat, and R. N. Zare, Chem. Phys. Lett. **63**, 217 (1979).
[8]F. Bylicki, M. Kolwas, and H. G. Weber, Phys. Rev. A **25**, 1550 (1982).
[9]F. Bylicki and H. G. Weber, Phys. Lett. **100A**, 182 (1984).
[10]C. Cohen-Tannoudji, in *Frontiers in Laser Spectroscopy,* edited by R. Balian, S. Haroche, and S. Liberman (North-Holland, Amsterdam, 1977), Vol. I.
[11]L. Allen and J. Eberly, *Optical Resonances and Two-Level Atoms* (Wiley, New York, 1975).
[12]T. Oka, in *Frontiers in Laser Spectroscopy,* edited by R. Balian, S. Haroche, and S. Liberman (North-Holland, Amsterdam, 1977), Vol. 2.
[13]R. W. Field, A. D. English, T. Tanaka, D. O. Harris, and D. A. Jennings, J. Chem. Phys. **59**, 2191 (1973).
[14]G. Miksch and H. G. Weber (unpublished).
[15]C. H. Chen, S. D. Kramer, D. W. Clark, and M. G. Payne, Chem. Phys. Lett. **65**, 419 (1979).
[16]A. E. Douglas, J. Chem. Phys. **45**, 1007 (1966).